

Novel Copper Fluoride Analogs of Cuprates

Nikita Rybin,¹ Dmitry Y. Novoselov,^{1,2,3} Dmitry M. Korotin,^{1,2} Vladimir I. Anisimov,^{1,2,3} and Artem R. Oganov¹

¹*Skolkovo Institute of Science and Technology, 30 Bolshoy Boulevard, bld. 1, Moscow 121205, Russia*

²*M. N. Mikheev Institute of Metal Physics of Ural Branch of Russian Academy of Sciences,*

18 S. Kovalevskaya St., Yekaterinburg 620137, Russia

³*Department of Theoretical Physics and Applied Mathematics,
Ural Federal University, 19 Mira St., Yekaterinburg 620002, Russia*

(Dated: August 31, 2020)

On the basis of the first-principles evolutionary crystal structure prediction of stable compounds in the CuF system, we predict two experimentally unknown stable phases – Cu₂F₅ and CuF₃. Cu₂F₅ comprises two interacting magnetic subsystems with the Cu atoms in the oxidation states +2 and +3. CuF₃ contains magnetic Cu³⁺ ions forming a lattice with the antiferromagnetic coupling. We showed that some or all of Cu³⁺ ions can be reduced to Cu²⁺ by electron doping, as in the well known KCuF₃. Significant similarities between the electronic structures calculated in the framework of DFT+U suggest that doped CuF₃ and Cu₂F₅ may exhibit high-*T_c* superconductivity with the same mechanism as in cuprates.

Transition metal fluorides have been thoroughly studied during the last century [1, 2]. Among them coinage metal fluorides recently attracted considerable attention: CuF system in the electrochemistry field [3–6], Ag-F as a potentially new route to superconductivity [7, 8], and Au-F due to the unusual oxidation state of gold [9]. Actually, Cu-F system contains an old puzzle of crystalline copper fluoride existence and synthesis, which produced a never-ending debate and remained unresolved to date. The first report of synthesis of CuF with zinblende structure was published in 1933 [10]. It was then argued that the reported CuF is identical to Cu₂O, dismissing the previous experimental results [11]. Recently no one succeeded in reproducing the synthesis of CuF, and the earliest studies have met strong criticism [12, 13], since it is commonly believed that fluorine, because of its high electronegativity, will always oxidize copper to the oxidation state +2. Even though all attempts to synthesize CuF have been unsuccessful and the very existence of this compound is questionable, studies are ongoing [14, 15], and the complexes of CuF are already well characterized [16].

The computationally guided studies of new transition metal fluorides, and CuF in particular, also continue. Initially, they mainly compared different structure prototypes to find a hypothetical ground state crystal structure [17, 18] or investigated cluster formation [19]. A variety of new structures have been reported using evolutionary crystal structure prediction and assuming CuF stoichiometry [20]. On the basis of all previous studies, eventually, it has been shown that all predicted structures are metastable [18, 20].

Recently, a computational crystal structure prediction of coinage metal fluorides at different pressures was done [9]. However, the used method works with a fixed stoichiometry, which limits the prediction of new phases in the whole system. Moreover, redoing the same calculations lead to different structures [21]. Thus, the detailed and reliable analysis of the whole Cu-F system remained to be done.

In this Letter, we present a first-principles variable-

composition evolutionary crystal structure prediction study of all phases in the CuF system. We recover the experimentally known structure of CuF₂ and report hitherto unknown stable *C2/m*-Cu₂F₅, *R3c*-CuF₃, and *Pnma*-CuF₃ phases. Based on the similarities between the crystal structure of the discovered fluorides and the structure of the parent cuprate high-temperature (high-*T_c*) superconductor La₂CuO₄, we explored the possibility of high-*T_s* superconductivity in doped copper fluorides.

Stable phases in the CuF system were predicted here using the first-principles evolutionary algorithm as implemented in the USPEX package [22, 23]. The evolutionary search was combined with structure relaxation and energy calculations using density functional theory (DFT) within the PerdewBurkeErnzerhof (PBE) [24] exchange-correlation functional and employing the projector augmented plane wave (PAW) method [25] as implemented in the VASP package [26]. We used the plane-wave energy cutoff of 600 eV and Γ -centered *k*-meshes with a resolution of $2\pi \times 0.05^{-1}$ for Brillouin zone sampling, ensuring excellent convergence of the quantities of interest. During the variable-composition structure search, the first generation of 160 structures was produced using random symmetric [27] and random topological [28] structure generators, with up to 18 atoms in the primitive cell. 70% of the next generation were obtained by applying variation operators (heredity, softmutation, lattice mutation) to the 70% of the lowest-energy structures of current generation and the other 30% of the generation were produced randomly.

Phases located on the thermodynamic convex hull are stable with respect to decomposition into elemental Cu and F or other CuF compounds. The spin-polarized DFT calculations lead to the convex hull diagram as presented on the (Fig. 1). It contains experimentally known *P2₁/c*-CuF₂, hitherto unknown *C2/m*-Cu₂F₅, *R3c*-CuF₃, and slightly metastable *Pnma*-CuF₃, which is just 0.001 eV above the convex hull. Successful prediction of the CuF₂, a known compound, indicates the robustness of our methodology. All obtained potentially stable struc-

tures became subject of an additional fixed-composition study taking into account up to four formula units (and up to 18 atoms in the unit cell for CuF). The dynamical stability of all structures was carefully verified with phonon calculations using the supercell approach and the finite displacement method, as implemented in the Phonopy package [29]. The structural information for the obtained compounds and results of the phonon calculations are presented in the Supporting Materials (SM).

The most energetically favorable structure of CuF, found in our study, is the low-symmetry $P1$ -CuF, which is even lower in energy than previous reports [20] by ~ 0.05 meV/atom, but its low symmetry and high energy (~ 50 meV/atom above the convex hull) indicated its instability and tendency to decompose into Cu+CuF₂. Thus, we conclude CuF is unlikely to exist at ambient pressure.

Cu₂F₅ crystallizes in the monoclinic space group $C2/m$ with two inequivalent Cu sites, where each Cu atom of the first type is bonded to six pairwise equivalent F atoms forming a CuF₆ octahedron (Fig. 2a), with the corner-sharing octahedral tilt angles of 0° . In the second site, the Cu atom is in a square planar geometry with four pairwise equivalent F atoms. This arrangement could be also described as a distorted octahedron (see SM Fig. 3a). While iso stoichiometric $P\bar{1}$ -Ag₂F₅ is well-known [7], hypothetical $P\bar{1}$ -Cu₂F₅ has a higher energy than $C2/m$ -Cu₂F₅ by ~ 3 meV/atom in the spin-polarized DFT solution.

Ground state CuF₃ has a trigonal perovskite structure with the space group $R\bar{3}c$ (Fig. 2b). This structure was also predicted in [9]. The Cu atom is bonded with six equivalent F atoms to form an octahedron with the corner-sharing octahedral tilt angles of 29° . Orthorhombic $Pnma$ -CuF₃, metastable at 0 K, also has a perovskite structure ABX₃ with absent A cations – ReO₃-type structure (Fig. 2c), with the corner-sharing octahedral tilt angles of 28° . Metal trifluorides FeF₃, CoF₃, RuF₃, RhF₃ PdF₃, and IrF₃ also have perovskite structure with the space group $R\bar{3}c$ [30], whereas AgF₃ and AuF₃ crystallize in a totally different structure with the space group $P6_122$ [31, 32]. Hypothetical $P6_122$ -CuF₃ has a higher energy than the $R\bar{3}c$ phase by ~ 30 meV/atom in the spin-polarized DFT solution. Notably, perovskite-type structures frequently have octahedral tilt instabilities and exhibit phase transition [33].

Discovered Cu fluorides have significant crystal-chemical similarities with high- T_s cuprates. In both systems we observe Cu⁺² (in square planar coordination, as a consequence of Jahn-Teller distortion in all cuprates and Cu₂F₅) and Cu⁺³ (in CuF₃, Cu₂F₅, and in doped cuprates). As we discuss below, pure parent compounds CuF₃, Cu₂F₅, and La₂CuO₄ are antiferromagnetic insulators, but doping by electrons or holes makes them metallic and superconducting (for sure La₂CuO₄, and most likely for copper fluorides).

To compare the electronic properties of copper fluorides and cuprate, we firstly performed

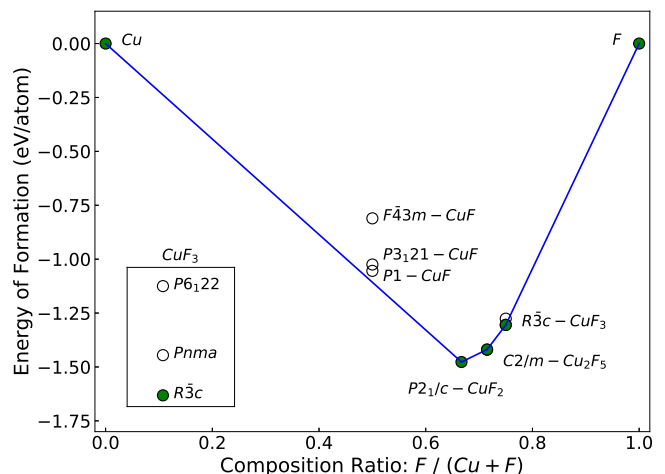


FIG. 1. Convex hull diagram of the CuF system. The inset schematically mentions existence of three CuF₃ phases.

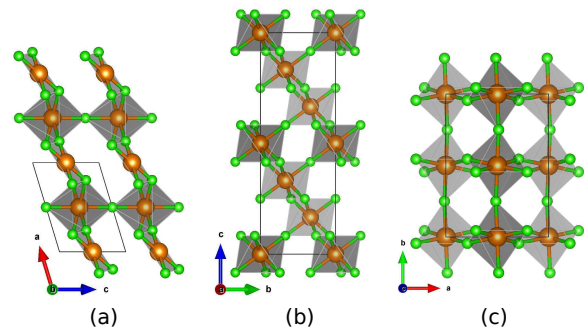


FIG. 2. (color online). Schematic representation of the crystal structures: (a) $C2/m$ -Cu₂F₅, (b) $R\bar{3}c$ -CuF₃, (c) $Pnma$ -CuF₃. The Cu and F atoms are shown in brown and green, respectively. Structures were visualized using VESTA software [34].

the spin-unpolarized DFT calculations using dense MonkhorstPack meshes of $8 \times 8 \times 4$ and $12 \times 12 \times 12$ kpoints for distorted orthorhombic low-temperature $Bamb$ -La₂CuO₄ phase and all fluorides, respectively. Structural information and energies for ferromagnetic and antiferromagnetic orders are presented in the (SM Tab.1, 2). The densities of states (DOS) for $R\bar{3}c$ -CuF₃, Cu₂F₅, and $Bamb$ -La₂CuO₄ resolved for the Cu-d and ligand-p states within DFT are shown on (Fig. 3a, c, e). In all systems DFT results show that the Cu-3d energy band is located completely inside the p band of the ligands and strongly hybridizes with it. Therefore, the partially filled electronic states of interest are formed by the d- and p-symmetry states with approximately equal weights, and the usual ionic picture is not applicable for such a band structure. Notably, the magnetic exchange interaction is proportion to the scale of magnetic fluctuations. For all considered systems, solutions with antiferromagnetic order are the lowest in energy (SM Tab.3, 4). Since the energy difference obtained from the spin-unpolarized and spin-polarized DFT calculations is quite small, one can

expect strong spin fluctuations in both types of systems – and we recall that high- T_c superconductivity of cuprates is believed to be mediated by spin fluctuations. Doped Cu fluorides can, or perhaps, even should be superconducting by the same magnetically mediated mechanism.

Although DFT shed light on some premature analogy with cuprates, in principle, this method is pathological since cannot correctly reproduce the antiferromagnetic insulating state of La_2CuO_4 because it neglects on-site Coulomb correlations [35], and more robust results are achieved by taking into account the electronic correlations using the DFT+U method with the Coulomb interaction parameter $U = 8$ eV and the exchange interaction parameter $J = 0.9$ eV [35, 36]. Because we deal with copper in the same divalent and trivalent states, and the energy bands in cuprates and copper fluorides studied here have similar widths (Fig. 3a, c, e and Tab. I), we chose the same values of U and J for all calculations taking into account the on-site Coulomb repulsion between the Cu-3d electrons in CuF_3 , Cu_2F_5 , and $\text{Bamb-La}_2\text{CuO}_4$. Structural information obtained after the relaxation with DFT+U as well as the values of total energy for ferromagnetic and antiferromagnetic orders are presented in the (SM Tab.1, 2).

We reproduced the insulating antiferromagnetic ground state of $\text{Bamb-La}_2\text{CuO}_4$ with the DFT+U energy gap of about 2 eV and the magnetic moment of the Cu atoms of $0.65 \mu_B$, which is in a close agreement with the experimentally observed values of ~ 2 eV and $0.68 \mu_B$, respectively [37]. The DOS for $R\bar{3}c\text{-CuF}_3$, Cu_2F_5 , and $\text{Bamb-La}_2\text{CuO}_4$ obtained using DFT+U are presented on (Fig. 3b, d, f). The DOS for $Pnma$ phase is presented on the (Fig. 2a, b in SM). For $R\bar{3}c\text{-CuF}_3$ and $Pnma\text{-CuF}_3$ in the antiferromagnetic phase, the DFT+U calculations show similarities in the key features of the electronic structures of CuF_3 and $\text{Bamb-La}_2\text{CuO}_4$ – they have well-separated Hubbard bands formed by the Cu-d states, whereas the first ionization states have a p-symmetry and are formed by the ligands.

In the CuF_3 structures, copper has an atypical formal oxidation state of +3, which leads to the $3d^8$ electronic configuration, whereas in $\text{Bamb-La}_2\text{CuO}_4$ there are Cu^{2+} JahnTeller active ions. However, some or all of Cu^{+3} ions in CuF_3 can be reduced to Cu^{+2} by electron doping, like in the well-known perovskite-type KCuF_3 , where all Cu atoms are in the oxidation state +2. CuF_3 , in fact, can be described as the structure of KCuF_3 with all K atoms removed. Thus, one way to make a superconducting Cu fluoride is to remove part of K atoms from KCuF_3 (in a vacuum tube) – the result should be a metallic perovskite-type compound with mixed Cu^{+2} and Cu^{+3} states. To clearly show this, we performed a fixed-composition structure search of $\text{K}_3(\text{CuF}_3)_4$, which determined that the most stable phase has perovskite-type structure with the space group $Im\bar{3}m$ (SM Fig. 3c). This structure is stable with respect to the decomposition into $R\bar{3}c\text{-CuF}_3$ and KCuF_3 (~ 0.05 eV/atom below the decomposition line), which means that potassium ions

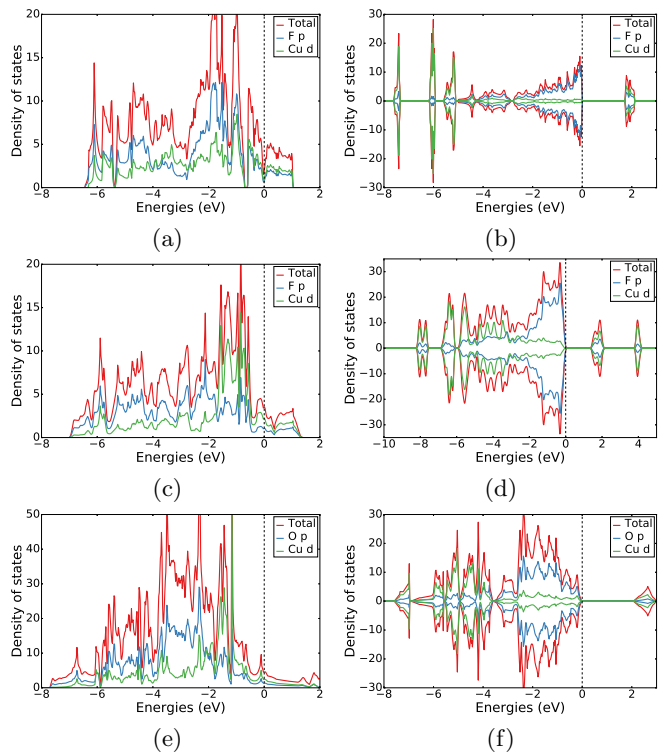


FIG. 3. (color online). Total and partial density of states for (a, b) $R\bar{3}c\text{-CuF}_3$, (c, d) Cu_2F_5 , and (e, f) $\text{Bamb-La}_2\text{CuO}_4$ obtained using (a, c, e) DFT and (b, d, f) DFT+U.

can be easily extracted from the KCuF_3 , forming mixed-valence compound.

TABLE I. Bandwidth W and charge transfer gap Δ_{pd} calculated using DFT. Hubbard bands splitting U_{dd} , spin S , and magnetic moment M obtained using the DFT+U method. The values in parentheses are related to the second type of Cu atoms in the Cu_2F_5 .

	W (eV)	Δ_{pd} (eV)	U_{dd} (eV)	S	M (μ_B)
$R\bar{3}c\text{-CuF}_3$	8	1.7	9.5	1	1.15
Cu_2F_5	8	1.42	9.5	1 (1/2)	1.17 (0.79)
La_2CuO_4	9	2	10.5	1/2	0.65

According to the DFT+U solution: each Cu site in the CuF_3 has spin 1; Cu_2F_5 is determined as a compound with the mixed-valence $\text{Cu}^{2+}/\text{Cu}^{3+}$ state and Cu ions with spin 1 and 1/2; Cu ions in the cuprate have spin 1/2. The magnetic moments per Cu atom obtained in the DFT+U calculations for $R\bar{3}c\text{-CuF}_3$ are $1.15 \mu_B$ ($1.14 \mu_B$ in the $Pnma$ phase). These magnetic moment values are smaller by a factor of 0.58 than the formal ionic value of $2 \mu_B$ for a Cu^{3+} ion compared to the reduction factor of 0.65 for the formal atomic value of $1 \mu_B$ for a Cu^{2+} ion in the La_2CuO_4 [37]. For Cu_2F_5 we found that two types of Cu atoms, have different formal electronic configurations, d^8 and d^9 , and different magnetic moments of $1.17 \mu_B$ and $0.79 \mu_B$. All predicted copper fluoride structures and $\text{Bamb-La}_2\text{CuO}_4$ are charge-transfer insulators

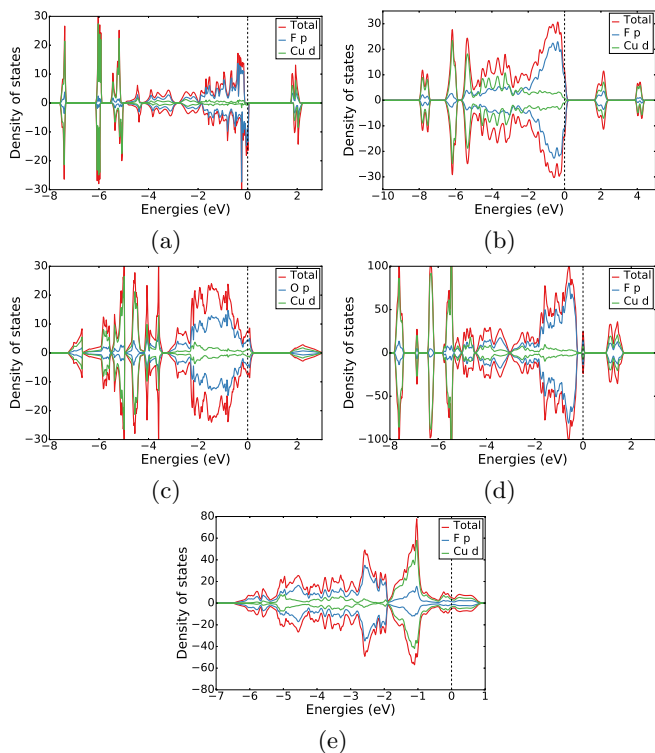


FIG. 4. (color online). Total and partial density of states for p-doped (a) $R\bar{3}c$ - CuF_3 , (b) Cu_2F_5 , and (c) La_2CuO_4 . (d) $R\bar{3}c$ - CuF_3 with the one F vacancy per $2 \times 2 \times 2$ supercell, (e) and perovskite-type $\text{Im}\bar{3}m$ - $\text{K}_3(\text{CuF}_3)_4$.

with respect to the classification of Zaanen *et al.* [38]. The first energy excitation occurs between the p band of the ligands and the d band of the metal ion. CuF_3 has a small charge transfer gap (an important characteristic of cuprates) $\Delta_{pd}=1.7$ eV, Cu_2F_5 also has a small charge transfer gap $\Delta_{pd}=1.42$ eV, comparable with 2 eV of La_2CuO_4 . Though the energy gap depends on the choice of the Hubbard U parameter, the charge-transfer nature of the gap remains the same for a wide range of U values in fluorides. The splitting between the Hubbard bands for CuF_3 and La_2CuO_4 is similar and equals to

~ 9.5 eV and 10.5 eV, respectively (Fig. 3b, d).

Cu_2F_5 , CuF_3 , and La_2CuO_4 are insulators and can display superconductivity only when properly doped. Consequently, we performed DFT+U calculations of the considered systems doped with holes using rigid-band shift approximation, with doping amounted to 0.25 holes for each copper atom in the unit cell (Fig. 4a, b, c). CuF_3 and Cu_2F_5 , like La_2CuO_4 , undergo a transition from the insulating to the conducting state upon the hole doping, which once again highlights the similarity of their electronic properties. We have also examined a $2 \times 2 \times 2$ $R\bar{3}c$ - CuF_3 supercell (64 atoms) with a vacancy on one of the F atoms. This ferrimagnetic structure lies on the thermodynamic convex hull (Fig. 1). This means that the formation of the non-stoichiometric CuF_{3-x} is favorable. The DFT+U solution determines the formation of a peak at the Fermi level for this structure (Fig. 4 d). Perovskite-type $\text{Im}\bar{3}m$ - $\text{K}_3(\text{CuF}_3)_4$ also has a metallic solution in DFT+U study (Fig. 4 e).

In summary, the results of the systematic crystal structure search in the CuF system supports that CuF is unlikely to exist and have revealed hitherto unknown $C2/m$ - Cu_2F_5 , $R\bar{3}c$ - CuF_3 , and slightly metastable $Pnma$ - CuF_3 . Cu_2F_5 contains Cu ions with oxidation states +2 and +3, which leads to the presence of two magnetic subsystems. In CuF_3 , Cu ions have an unusual oxidation state +3, which can be reduced to +2 by proper doping. We showed that potassium can be extracted from KCuF_3 forming metallic state. we showed using DFT+U that all discovered copper fluorides are strongly correlated compounds and charge-transfer insulators. Since comparison of the CuF_3 and Cu_2F_5 with the classical cuprate La_2CuO_4 shows many similarities, discovered structures possibly could be a new class of high- T_c superconductors.

Acknowledgments. This work was supported by the Russian Science Foundation (Project 19-72-30043). Calculations were performed on Arkuda cluster of Skoltech and Uran cluster of IMM UB RAS. DYN, DMK and VIA thanks the Ministry of Science and Higher Education of the Russian Federation (No. AAAA-A18-118020190098-5, topic "Electron").

-
- [1] J. M. Winfield, *Journal of Fluorine Chemistry* **33**, 159 (1986).
 [2] J. S. Thrasher and S. H. Strauss, "Inorganic Fluorine Chemistry," in *Inorganic Fluorine Chemistry* (1994) Chap. 1, pp. 1–23.
 [3] F. Wang, R. Robert, N. A. Chernova, N. Pereira, F. Omenya, F. Badway, X. Hua, M. Ruotolo, R. Zhang, L. Wu, V. Volkov, D. Su, B. Key, M. Stanley Whittingham, C. P. Grey, G. G. Amatucci, Y. Zhu, and J. Graetz, *Journal of the American Chemical Society* **133**, 18828 (2011).
 [4] F. Wang, H. C. Yu, M. H. Chen, L. Wu, N. Pereira, K. Thornton, A. Van Der Ven, Y. Zhu, G. G. Amatucci, and J. Graetz, *Nature Communications* **3**, 1 (2012).
 [5] X. Hua, R. Robert, L.-S. Du, K. M. Wiaderek, M. Leskes, K. W. Chapman, P. J. Chupas, and C. P. Grey, *The Journal of Physical Chemistry C* **118**, 15169 (2014).
 [6] F. Omenya, N. J. Zagarella, J. Rana, H. Zhang, C. Siu, H. Zhou, B. Wen, N. A. Chernova, L. F. J. Piper, G. Zhou, and M. S. Whittingham, *ACS Applied Energy Materials* **2**, 5243 (2019).
 [7] W. Grochala and R. Hoffmann, *Angewandte Chemie International Edition* **40**, 2742 (2001).
 [8] J. Gawraczynski, D. Kurzydowski, R. A. Ewings, S. Bandaru, W. Gadomski, Z. Mazej, G. Ruzani, I. Bergenti, T. Jaron, A. Ozarowski, S. Hill, P. J. Leszczynski, K. Tokár, M. Derzsi, P. Barone, K. Wohlfeld, J. Lorenzana, and W. Grochala, *Proceedings of the National Academy of Sciences of the United States of America* **116**, 11111 (2019).
 [9] J. Lin, S. Zhang, W. Guan, G. Yang, and Y. Ma,

- Journal of the American Chemical Society **140**, 9545 (2018).
- [10] F. Ebert and H. Woitinek, *Zeitschrift für anorganische und allgemeine Chemie* **210**, 269 (1933).
- [11] H. M. Haendler, L. H. Towle, E. F. Bennett, and W. L. Patterson, *Journal of the American Chemical Society* **76**, 2178 (1954).
- [12] C. Housecroft and A. Sharpe, *Inorganic Chemistry* (Pearson Prentice Hall, 2005).
- [13] N. N. Greenwood and A. Earnshaw, *Chemistry of the Elements* (Elsevier Science, 2012).
- [14] X. Wang, L. Andrews, F. Brosi, and S. Riedel, *Chemistry A European Journal* **19**, 1397 (2013).
- [15] P. Woidy, A. J. Karttunen, M. Widemeyer, R. Niewa, and F. Kraus, *Chemistry A European Journal* **21**, 3290 (2015).
- [16] D. J. Gulliver, W. Levason, and M. Webster, *Inorganica Chimica Acta* **52**, 153 (1981).
- [17] T. Söhnel, H. Hermann, and P. Schwerdtfeger, *Journal of Physical Chemistry B* **109**, 526 (2005).
- [18] A. Walsh, C. R. A. Catlow, R. Galvelis, D. O. Scanlon, F. Schiffmann, A. A. Sokol, and S. M. Woodley, *Chemical Science* **3**, 2565 (2012).
- [19] R. P. Krawczyk, A. Hammerl, and P. Schwerdtfeger, *ChemPhysChem* **7**, 2286 (2006).
- [20] M. S. Kuklin, L. Maschio, D. Usvyat, F. Kraus, and A. J. Karttunen, *Chemistry A European Journal* **25**, 11528 (2019).
- [21] G. Liu, X. Feng, L. Wang, S. A. Redfern, X. Yong, G. Gao, and H. Liu, *Physical Chemistry Chemical Physics* **21**, 17621 (2019).
- [22] A. R. Oganov and C. W. Glass, *The Journal of Chemical Physics* **124**, 244704 (2006).
- [23] A. R. Oganov, A. O. Lyakhov, and M. Valle, *Accounts of Chemical Research* **44**, 227 (2011).
- [24] P. Perdew, K. Burke, and M. Ernzerhof, *Physical Review Letters* **77**, 3865 (1996).
- [25] P. E. Blöchl, *Physical Review B* **50**, 17953 (1994).
- [26] G. Kresse and J. Furthmüller, *Physical Review B* **54**, 11169 (1996).
- [27] A. O. Lyakhov, A. R. Oganov, H. T. Stokes, and Q. Zhu, *Computer Physics Communications* **184**, 1172 (2013).
- [28] P. V. Bushlanov, V. A. Blatov, and A. R. Oganov, *Computer Physics Communications* **236**, 1 (2019).
- [29] *Scripta Materialia* **108**, 1 (2015).
- [30] M. A. Hepworth, K. H. Jack, R. D. Peacock, and G. J. Westland, *Acta Crystallographica* **10**, 63 (1957).
- [31] B. Žemva, K. Lutar, A. Jesih, W. J. Cas-teel, A. P. Wilkinson, D. E. Cox, B. Robert von Dreele, H. Borrmann, and N. Bartlett, *Journal of the American Chemical Society* **113**, 4192 (1991).
- [32] F. W. Einstein, P. R. Rao, J. Trotter, and N. Bartlett, *Journal of the Chemical Society A: Inorganic, Physical, and Theoretical Chemistry* **1957**, 100 (1957).
- [33] P. M. Woodward, *Acta Crystallographica Section B* **53**, 32 (1997).
- [34] K. Momma and F. Izumi, *Journal of Applied Crystallography* **41**, 653 (2008).
- [35] M. T. Czyzyk and G. A. Sawatzky, *Physical Review B* **49**, 14211 (1994).
- [36] V. I. Anisimov, F. Aryasetiawan, and A. I. Lichtenstein, *Journal of Physics Condensed Matter* **9**, 767 (1997).
- [37] W. E. Pickett, *Reviews of Modern Physics* **61**, 433 (1989).
- [38] J. Zaanen, G. A. Sawatzky, and J. W. Allen, *Physical Review Letters* **55**, 418 (1985).